RSC Advances

Fe3O4@chitosan nanoparticles: a valuable heterogeneous nanocatalyst for the synthesis of 2,4,5-trisubstituted imidazoles

Journal:	*RSC Advances*
Manuscript ID:	RA-ART-04-2014-003176
Article Type:	Paper
Date Submitted by the Author:	08-Apr-2014
Complete List of Authors:	zarnegar, zohre; university of kashan, chemistry safari, javad; University of Kashan, Organic Chemistr

Cite this: DOI: 10.1039/c0xx00000x

www.rsc.org/xxxxxx

ARTICLE TYPE

Fe_3O_4@chitosan nanoparticles: a valuable heterogeneous nanocatalyst for the synthesis of 2,4,5-trisubstituted imidazoles

Zohre Zarnegar, Javad Safari*

Laboratory of Organic Compound Research, Department of Organic Chemistry, College of Chemistry, University of Kashan, P.O. Box: 87317-51167, Kashan, I.R., Iran.Corresponding author. E-mail addresses: Safari@kashanu.ac.ir; safari_jav@yahoo.com. , Tel: +98 361 591 2320; Fax: +98 361 5912397.

Received (in XXX, XXX) Xth XXXXXXXXX 20XX, Accepted Xth XXXXXXXXX 20XX
DOI: 10.1039/b000000x

Chitosan-coated Fe_3O_4 nanoparticles (Fe_3O_4@CS) were prepared simply through in situ co-precipitation of Fe^{2+} and Fe^{3+} ions via NH_4OH in an aqueous solution of chitosan and its catalytic activity was investigated in the synthesis of 2,4,5-trisubstituted imidazoles by a one-pot condensation of benzil derivatives, aryl aldehydes and ammonium acetate in EtOH. This novel method offers several advantages compared to those reported in the previous literatures, including avoiding the use of harmful catalysts, easy and quick isolation of the products, excellent yields, mild and clean conditions, and simplicity of the methodology. High catalytic activity and ease of recovery using an external magnetic field are additional eco-friendly attributes of this catalytic system.

1. Introduction

Imidazole derivatives are a class of heterocyclic compounds that contain nitrogen and are currently under intensive focus due to their wide range of applications, because they have many pharmacological properties and play important roles in biochemical processes.[1,2] The imidazole compounds are known to possess NO synthase inhibition and antifungal, antibiotic, antimycotic, antiulcerative, antitumor, antibacterial, and CB1 receptor antagonistic activities.[3,4] Various substituted imidazoles act as inhibitors of p38 MAP kinase[5] and B-Raf kinase,[6] plant growth regulators,[7] glucagon receptors,[8] pesticides,[9] and therapeutic agents.[10] Thus, synthesis of these important heterocyclic nucleus have rekindled our interest in obtaining trisubstituted imidazole. Accordingly, a number of synthetic methods have been reported for the synthesis of 2,4,5-trisubstituted imidazoles. These methods involve condensation of aldehyde, benzil and ammonium acetate by using various catalytic systems.[11-18] Owing to the wide range of pharmacological and biological activities, the development of economical, effective, clean, high-yielding and mild environmental benign protocols is still desirable and is in demand. Moreover, the design of efficient, valuable, and recoverable catalysts is important for both economical and environmental points of view.

In recent decade, magnetic nanoparticles (MNPs) have appeared as an excellent type of catalyst support because of their good stability, easy synthesis and functionalization, high surface area and facile separation by magnetic forces, as well as low toxicity and price.[19] Other important features of these magnetic catalysts are high catalytic activity, simple magnetic separation of them using an external magnet, high degree of chemical stability in various organic and inorganic solvents, reusability and benign character in the context of green chemistry. As a result, magnetically recyclable nanocatalyst systems have enabled researchers to apply nanocatalysts as greener and sustainable options for organic transformations.[20]

On the other hand, recently biopolymers such as cellulose,[21] starch,[22] chitosan (CS)[20,23] or wool[24] have been used as heterogeneous catalytic systems. In this context, chitosan can play a major role as a natural, biocompatible, and biodegradable polymer. Literature survey shows that a wide range of applications have been reported for chitosan in different fields such as drug delivery, cosmetics, water treatment, food packaging, fuel cells, membranes, hydrogels, surface conditioners, and catalyst.[25] Chitosan as a polyaminosaccharide, can be explored as a mild bifunctional heterogeneous catalyst in organic reactions. In this regard, chitosan contains both amino groups and primary and secondary hydroxyl groups in higher concentrations. Therefore, chitosan can activate the electrophilic and nucleophilic components of the reactions by hydrogen bonding and lone pairs, respectively.[23a]

< Scheme 1. >

Herein we wish to report a new efficient and practical route for the one-pot three-component synthesis of trisubstituted imidazoles by the condensation of benzil derivatives, aryl aldehydes and ammonium acetate catalyzed by Fe_3O_4@CS nanoparticles. This new approach has several superiorities versus previous reports for the synthesis of highly substituted imidazole derivatives and opens an important field to the use of magnetically recoverable and environmentally benign heterogeneous nanocatalyst in the synthesis of pharmaceutically important heterocyclic compounds (Scheme 1)..

< Scheme 1>

2. Results and discussion

Fe_3O_4 nanoparticles are prepared by chemical co-precipitation of Fe^{2+} and Fe^{3+} ions with molar ratio 1:2, in presence of chitosan, followed by the hydrothermal treatment (scheme 2).

<Scheme 2>

The magnetically heterogeneous catalyst, Fe_3O_4@CS nanoparticles, is characterized by FT-IR (Fig. 1), XRD (Fig. 2), TGA (Fig. 3), SEM (Fig. 4), and VSM (Fig. 5). The FT-IR spectra of chitosan, Fe_3O_4, and Fe_3O_4@CS, consistent with their respective structures (Fig. 1). The FT-IR spectrum of chitosan (Fig. 1(a)) shows a broad band at 3433 cm^{-1} which corresponds to the stretching vibrations of O-H and N-H groups. Peaks appearing at 2923 and 2855 cm^{-1} are characteristic of C-H stretching vibrations. The band at 1634 cm^{-1} is assigned to N-H bending vibration and that of 1423 cm^{-1} to C-O stretching of primary alcoholic groups in chitosan. The band at 1084 cm^{-1} display the stretching vibrations of the C-O bond. The Fe–O stretching vibration near 576 cm^{-1}, O–H stretching vibration near 3429 cm^{-1}, O-H deformed vibration near 1620 cm^{-1} were observed for Fe_3O_4 MNPs in Fig. 1(b). For Fe_3O_4@CS nanoparticles, chitosan absorptions appear in additionto a peak at 580 cm^{-1} which corresponds to the stretching vibration of Fe-O groups; indicating that the magnetic Fe_3O_4 MNPs are coated by chitosan (Fig. 1(c)).[20]

< **Fig. 1**. >

To confirm the presence of crystalline Fe_3O_4 and Fe_3O_4@chitosan nanoparticles, the structure of the magnetic nanoparticles was characterized by XRD and the diffractogram is shown in Fig. 2. There are eight diffraction peaks: (2 2 0), (3 1 1), (4 0 0), (3 3 1) (4 2 2), (3 3 3), (4 4 0) and (5 3 1) in the Fe_3O_4 and Fe_3O_4@chitosan, which is the standard pattern for crystalline magnetite with spinel structure (JCPDS card No. 01-1111).[27] It is clearly seen there is little influence of the dispersant on the structure of magnetic particles, except that the amorphous phase of chitosan appears as a scattered maximum on the background as seen from Fig. 2(b). As shown in Fig. 2(b), the XRD patterns confirm that the coating process did not induce any phase change of Fe_3O_4 MNPs.

In order to obtain information on the thermal stability, TGA experiments are carried out by heating Fe_3O_4 and Fe_3O_4@CS up to 600 °C (Fig. 3). The weightloss of Fe_3O_4@CS nanoparticles is about 40% at 250–350 °C, correspondingto the thermal decomposition of chitosan chains over Fe_3O_4 nanoparticles.[26]

< **Fig. 2**>

< **Fig. 3**>

As illustrated in Fig. 4, the particle size was studied by scanning electron microscopy (SEM) and the identification of Fe_3O_4@chitosan was based on the analysis of SEM images. The obtained SEM images of nanoparticles clearly showed that Fe_3O_4 nanoparticles were properly supported on chitosan.

< **Fig. 4**>

Magnetic measurements of Fe_3O_4 and Fe_3O_4@chitosan nanoparticles were investigated with VSM. The hysteresis loops of Fe_3O_4 and Fe_3O_4@chitosan nanoparticles are shown in Fig. 5. It can be seen that both materials show ferromagnetic behavior. The magnetic saturation values of Fe_3O_4 MNPs and Fe_3O_4@chitosan nanoparticles are 66.58 and 20.17 emu g^{-1}, respectively. The decrease in magnetic saturation for Fe_3O_4@chitosan is attributed to the cover of chitosan polymeric matrix on the surface of magnetic Fe_3O_4 MNPs.[28] However, such a magnetic property is strong enough for the as-prepared Fe_3O_4@chitosan to be easily separated from EtOH under a magnetic field. The magnetic effect of Fe_3O_4@chitosan under an external magnetic field is shown in Fig. 6. Clearly, the Fe_3O_4@chitosan can be easily and quickly separated from the reaction mixture with the help of an external magnet, which proves that magnetic property of the Fe_3O_4@chitosan as nanocatalyst is strong enough for easy recovery and reuse from the reaction mixture.

< Fig. 5>

< Fig. 6>

To show the efficiency of the Fe_3O_4@chitosan as magnetic catalyst, initially, we sought a mild and convenient method for the synthesis of 2,4,5-trisubstituted imidazole derivatives at heating condition. Our investigation began with the evaluation of Fe_3O_4@chitosan as heterogeneous catalyst in the reaction of benzaldehyde (1 mmol), benzil (1 mmol) and ammonium acetate (5 mmol) as model reaction. The use of 0.05 g of Fe_3O_4@chitosan as nanocatalyst in EtOH afforded a 95% yield (Table 1, entry 4) of the desired product **4a**. Among the tested solvents such as chloroform, dichloromethane, methanol, ethanol, and acetonitrile, the formation of product **4a** was more facile and proceeded to give highest yield, in EtOH as solvent. The results indicated that the yield gradually decreased as we moved from highly polar to less polar solvents. To evaluate and optimize the catalytic system, one-pot condensation to give **4a** was examined with Fe_3O_4, chitosan Fe_3O_4@chitosan as catalyst (Table 1). Interestingly, it was found that Fe_3O_4@chitosan was proved to be an efficient catalyst and gave exclusively 1-(phenyl)-2,4,5-triphenylimidazole **4a** in 95% yield in 2 h under reflux conditions. (Table 1). As Table 1 shows, initial screening studies identified that all the above-mentioned catalysts shows a good catalytic activity for the model reaction but Fe_3O_4@chitosan exhibited highest catalytic activity as compared with Fe_3O_4 and chitosan. We believe that this composite has two active components for catalytic activity containing chitosan and magnetite. With notice to these results, Fe_3O_4@chitosan were chosen as the best catalyst for further work.

< **Table 1**>

We next examined a wide variety of aldehydes and 1,2-diketones to establish the scope of this catalytic transformation (Table 2). Various aromatic aldehydes bearing electron donating and electron withdrawing substituents underwent this cyclocondensation to furnish trisubstituted imidazoles in high yields. Also, benzil derivatives afforded the corresponding imidazoles in high yields. In general, this synthetic protocol was clean and no side products were detected. In all cases, the reactions proceeded efficiently under mild conditions. The results reveal that the unique heterogeneous Fe_3O_4@chitosan nanoparticles appears as an effective catalyst which produces high yields through a simple procedure.

< **table 2**>

The structure of trisubstituted imidazoles **4a–4l** was deduced fromtheir high-field ^{1}HNMR, IR, Rf, and UV spectral data. Also,

their melting points were compared with literature reports. ^{1}H NMR spectra for compound **4b** is given in Fig. 6. In the ^{1}H NMR spectra Fig 6(a), the signal around δ=3.0 ppm corresponding to methoxy group, In this figure, the signals of aromatic protons can be seen at δ=7.4-8.1 ppm. The signal around δ=12.5 ppm is related to the NH proton. Presence of this signal confirmed the formation of desired products in this reaction. To prove NH group, we have investigated hydrogen-deuterium exchange protocol for compound **4b** (Fig. 6(b)). In this method, a drop of D_2O is placed in the NMR tube containing the Acetone solution of the compound **4b.** After shaking a sample and sitting for a few minutes, the NH hydrogen is replaced deuterium, causing it to disappear from the spectrum at δ=12.5 ppm.

<Fig. 6>

A plausible mechanism for this reaction catalyzed by Fe_3O_4@chitosan is shown in scheme 3. In the case of trisubstituted imidazole the reaction proceeds through diamine intermediate A. The aldehydic carbonyl oxygen are activated by Fe_3O_4 (Fe^{+3} and Fe^{+2}) and chitosan supported magnetic nanoparticles and subsequent condensation with two molecules of ammonia to form diamine intermediate A. The free hydroxyl and amino groups distributed on the surface of chitosan supported Fe_3O_4 in high concentrations activate the carbonyl group of the aldehyde.[23a] Condenses with the carbonyl carbons of the 1,2-diketone followed by dehydration to afford the imino intermediate B, which rearranges to the required trisubstituted imidazoles.[1]

< scheme 3>

One of the advantages of this active, non-toxic, and environmentally benign heterogeneous bio-polymer catalyst is its ability to perform as a recyclable reaction medium. In a typical procedure, after completion of the reaction, the magnetic nanocatalyst is easily and efficiently separated from the product by attaching an external magnet to the reaction vessel, followed by simple decantation of the reaction solution (Fig. 7). The recycled catalyst could be reused six times without great loss of catalytic activity (Fig. 8). The recovered nanocatalyst was characterized with FT-IR spectroscopy (Fig. 1(d)). In IR spectrum, the band from 580 cm^{-1} is assigned to the stretching vibrations of (Fe-O) bond in Fe_3O_4, and the band at about 1027 cm^{-1} is belong to the stretching of the (C-O) bond. The coated cross-linked chitosan ensured the stability of the Fe_3O_4 core during the catalytic process, so as to obtain a high recyclability. After 6 times of reuse, chitosan may be destroyed and Fe_3O_4 having lost the protection of chitosan was easy to aggregate (as shown in SEM image Fig. 4(c)) or oxidize. There for, the catalyst would be lost in the solution and recovery efficiency decreased gradually.[23b]

< Fig.7>

< Fig.8>

3. Conclusions

In summary, a new, simple, efficient and environmentally benign method for the synthesis of 2,4,5-trisubstituted imidazoles by the use of renewable and heterogeneous Fe_3O_4@chitosan as magnetic biocatalyst has been described. Clean reaction profiles, excellent yields, the use of a one-pot and multicomponent procedure for the synthesis of imidazoles, reusability of the catalyst, practicability, and operational simplicity are the important features of this methodology.

4. Experimental

4.1. Chemicals and apparatus

All reagents were purchased from Merck and Aldrich and used without further purification. Melting points were determined in open capillaries using an Electrothermal Mk3 apparatus and are uncorrected. ^{1}H NMR and ^{13}C NMR spectra were recorded with a Bruker DRX-400 spectrometer at 400 and 100 MHz respectively. NMR spectra were obtained in DMSO-d_6 and acetone solutions and are reported as parts per million (ppm) downfield from tetramethylsilane as internal standard. Fourier transform infrared spectroscopy (FT-IR) spectra were obtained with potassium bromide pellets in the range 400-4000 cm^{-1} with a Perkin–Elmer 550 spectrometer. The UV–vis measurements were obtained with a GBC cintra 6 UV–vis spectrophotometer. Nanostructures were characterized using a Holland Philips Xpert X-ray powder diffraction (XRD) diffractometer (CuK, radiation, λ = 0.154056 nm), at a scanning speed of 2°/min from 10° to 100° (2θ). Scanning electron microscope (SEM) was performed on a FEI Quanta 200 SEM operated at a 20 kV accelerating voltage. The samples for SEM were prepared by spreading a small drop containing nanoparticles onto a silicon wafer and being dried almost completely in air at room temperature for 2 h, and then were transferred onto SEM conductive tapes. The transferred sample was coated with a thin layer of gold before measurement. The magnetic properties were characterized by a vibrating sample magnetometer (VSM, Lakeshore7407) at room temperature.

4.2. Preparation of the Fe_3O_4@CS

Fe_3O_4@CS nanoparticles were prepared using chemical coprecipitation described in the literature.[26] In short, 1.5 g of chitosan (molecular weight: 100,000–300,000) is dissolved in 100 mL of 0.05 M acetic acid solution; to which $FeCl_2{\cdot}4H_2O$ (1.29 g, 0.0065 mol) and $FeCl_3{\cdot}6H_2O$ (3.51 g, 0.013 mol) are added. The resulting solution is mechanically stirred for 6 h at 80 °C under Ar atmosphere. Subsequently, 6 mL of 25% NH_4OH is injected dropwise into the reaction mixture with constant stirring. After 30 min, the mixture is cooled to room temperature and chitosan coated over magnetic nanoparticles were separated by magnetic decantation and washed three times with distilled water, then ethanol, and finally dried under vacuum at room temperature (Scheme 3).

4.3. General procedure for the synthesis of 2,4,5-trisubstituted imidazoles

A mixture of benzil (1 mmol), aldehyde (1 mmol), ammonium acetate (0.4 g, 5 mmol) and Fe_3O_4@CS (0.05 g) in 10 mL ethanol was taken in a 50 mL flask and the reaction mixture was stirred under reflux condition for the stipulated period of time. The progress of the reaction was monitored by TLC. After the reaction was completed, the catalyst was separated by an external magnet. The reaction mixture was concentrated on a rotary evaporator under reduced pressure and the solid product obtained

was washed with water and recrystallized from acetone–water 9:1 (v/v) to produce the desired 2,4,5-trisubstituted imidazoles.

4.4. Product characterization data of 2,4,5-trisubstituted imidazoles

4.4.1. *2,4,5-triphenyl-1H-imidazol* (**4a**, $C_{21}H_{16}N_2$)

White powder; R_f (in petroleum ether:ethylacetate; 7:3(v/v)): 0.74; U.V ($CHCl_3$) λ_{max}(nm) : 334; IR (KBr) $\bar{\nu}$ (cm^{-1}) : 3434 (N-H),1597 (C=C), 1490 (C=N), ^{1}H NMR (Acetone+DMSO-d_6, 400 MHz) δ (ppm): 12.9 (s, 1H, N-H), 8.63 (d, 2H, ^3J=7.9 Hz, Ar-H), 8.08-7.14 (m, 4H, Ar-H), 7.92 (m, 4H, Ar-H), 7.83 (t, ^3J=8 Hz, 2H, Ar-H), 7.73 (t, ^3J=7 Hz, 2H, Ar-H), 7.67 (t, ^3J=8 Hz, 1H, Ar-H).

4.4.2. *2-(4-methoxyphenyl)-4,5-diphenyl-1H-imidazole (**4b**, $C_{22}H_{18}N_2O$)*

White powder; R_f (in petroleum ether:ethylacetate; 7:3(v/v)): 0.64; U.V ($CHCl_3$) λ_{max}(nm) : 338; IR (KBr) $\bar{\nu}$ (cm^{-1}): 3432 (N-H), 1611 (C=C), 1494 (C=N), 1250 (C-O); ^{1}H NMR (Acetone+DMSO-d_6, 400 MHz) δ (ppm): 12.5 (s, 1H, N-H), 8.12 (d, 2H, ^3J=8.8 Hz, Ar-H), 7.58-7.59 (m, 4H, Ar-H), 7.30-7.36 (m, 6H, Ar-H), 7.04 d, 2H, ^3J=8.4 Hz, Ar-H), 3.85 (s, 3H, OCH_3).

4.4.3. *2-(3,4-dimethoxyphenyl)-4,5-diphenyl-1H-imidazole (**4c**, $C_{23}H_{20}N_2O_2$)*

White powder; R_f (in petroleum ether:ethylacetate; 7:3(v/v)): 0.23; U.V ($CHCl_3$) λ_{max}(nm): 350; IR (KBr) $\bar{\nu}$ (cm^{-1}): 3430 (N-H), 1600 (C=C), 1500 (C=N), 1257 (C-O); ^{1}H NMR ($CDCl_3$, 400 MHz) δ (ppm): 9.8 (s, 1H, N-H), 8.53-8.58 (m, 3H, Ar-H), 7.27-7.33 (m, 9H, Ar-H), 6.90 (d, 1H, ^3J=7.6 Hz, Ar-H), 3.92 (s, 3H, OCH_3), 3.89 (s, 3H, OCH_3).

4.4.4. *2-(4-chlorophenyl)-4,5-diphenyl-1H-imidazole (**4d**, $C_{21}H_{15}N_2Cl$)*

White powder; R_f (in petroleum ether:ethylacetate; 7:3(v/v)): 0.86; U.V ($CHCl_3$) λ_{max}(nm) : 348; IR (KBr) $\bar{\nu}$ (cm^{-1}): 3433 (N-H), 1602 (C=C), 1485 (C=N), ^{1}H NMR ($CDCl_3$, 400 MHz) δ (ppm): 9.6 (s, 1H, N-H), 7.83-7.85 (d, 2H, ^3J=8.4 Hz, Ar-H), 7.56 (m, 4H, Ar-H), 7.41-7.43 (d, 2H, ^3J=8.4 Hz, Ar-H), 7.27-7.37 (m, 6H, Ar-H).

4.4.5. *2-(3-methoxyphenyl)-4,5-diphenyl-1H-imidazole (**4e**, $C_{22}H_{18}N_2O$)*

White powder; R_f (in petroleum ether:ethylacetate; 7:3(v/v)): 0.37; U.V ($CHCl_3$) λ_{max}(nm): 346; IR (KBr) $\bar{\nu}$ (cm^{-1}): 3435 (N-H), 1591 (C=C), 1482 (C=N), 1241 (C-O); ^{1}H NMR ($CDCl_3$, 400 MHz) δ (ppm): 9.5 (s, 1H, N-H), 7.54 (m, 1H, Ar-H), 7.43-7.27 (m, 11H, Ar-H), 6.95 (d, 1H, ^3J=8 Hz, Ar-H), 3.89 (s, 3H, OCH_3).

4.4.6. *2-(2-naphthyl)-4,5-diphenyl-1H-imidazole (**4f**, $C_{28}H_{18}N_2$)*

White powder; R_f (in petroleum ether:ethylacetate; 7:3(v/v)): 0.79; U.V ($CHCl_3$) λ_{max}(nm): 344, IR (KBr) $\bar{\nu}$ (cm^{-1}) : 3434 (N-H),1631 (C=C), 1501 (C=N), ^{1}H NMR ($CDCl_3$, 400 MHz) δ (ppm): 9.6 (s, 1H, N-H), 8.37 (s, 1H, Ar-H), 8.1 (d, 1H, ^3J=8 Hz, Ar-H),7.76-7.95 (m, 3H, Ar-H), 7.61 (m, 3H, Ar-H), 7.52-7.53 (t, 3H, ^3J=7.6 Hz, Ar-H), 7.34-7.38 (m, 6H, Ar-H).

4.4.7. *2-(3,5-dimethoxyphenyl)-4,5-diphenyl-1H-imidazole (**4g**, $C_{23}H_{20}N_2O_2$)*

White powder; R_f (in petroleum ether:ethylacetate; 7:3(v/v)): 0.37; U.V ($CHCl_3$) λ_{max}(nm): 344, IR (KBr) $\bar{\nu}$ (cm^{-1}): 3434 (N-H), 1601 (C=C), 1470 (C=N), 1155 (C-O); ^{1}H NMR (Acetone+DMSO-d_6, 400 MHz) δ (ppm): 12.9 (s, 1H, N-H), 8.01-8.07 (m, 4H, Ar-H), 7.83-7.88 (m, 5H, Ar-H), 7.78 (d, 2H, ^3J=7.8 Hz, Ar-H), 7.64 (t, 1H, ^4J=2 Hz, Ar-H), 3.31 (s, 6H, OCH_3).

4.4.8. *2-(phenyl)-4,5-bis(4-methoxyphenyl)-1Himidazole (**4h**, $C_{23}H_{20}N_2O_2$)*

White powder; R_f (in petroleum ether:ethylacetate; 7:3(v/v)): 0.62U.V ($CHCl_3$) λ_{max}(nm): 344; IR (KBr) $\bar{\nu}$ (cm^{-1}): 3430 (N-H), 1613 (C=C), 1504 (C=N), 1248 (C-O); ^{1}H NMR (Acetone+DMSO-d_6, 400 MHz) δ (ppm): 12.7 (s, 1H, N-H), 8.62 (d, 2H, ^3J=7.2 Hz, Ar-H), 7.87-7,97 (m, 7H, Ar-H); 7.80 (d, 1H, ^3J=7.2 Hz, Ar-H), 7.38-7.42 (m, 3H, Ar-H), 4.27 (s, 6H, OCH_3).

4.4.9. *2-(4-methoxyphenyl)-4,5-bis(4-methoxyphenyl)-1H-imidazole (**4i**, $C_{24}H_{22}N_2O_3$)*

White powder; R_f (in petroleum ether:ethylacetate; 7:3(v/v)): 0.28; U.V ($CHCl_3$) λ_{max}(nm): 348, IR (KBr) $\bar{\nu}$ (cm^{-1}): 3426 (N-H), 1612 (C=C), 1507 (C=N), 1261 (C-O); ^{1}H NMR (Acetone+DMSO-d_6, 400 MHz) δ (ppm): 12.7 (s, 1H, N-H), 8.53 (d, 2H, ^3J=8.8 Hz, Ar-H), 7.92-7.97 (m, 4H, Ar-H), 7.47 (m, 4H, Ar-H), 7.33 (d, 2H, ^3J=8 Hz, Ar-H), 4.29 (s, 9H, $3OCH_3$).

4.4.10. *2-(2-naphthyl)-4,5-bis(4-methoxyphenyl)-1H-imidazole (**4j**, $C_{27}H_{22}N_2O_2$)*

Cream powder; R_f (in petroleum ether:ethylacetate; 7:3(v/v)): 0.48; U.V ($CHCl_3$) λ_{max}(nm): 360; IR (KBr) $\bar{\nu}$ (cm^{-1}): 3425 (N-H), 1613 (C=C), 1511 (C=N), 1247(C-O); ^{1}H NMR (DMSO-d_6, 400 MHz) δ (ppm): 12.7 (s, 1H, N-H), 8.56 (s, 1H, Ar-H), 8.22 (d, 1H, ^3J=8 Hz, Ar-H), 7.96-7.98 (m, 4H, Ar-H), 7.46-7.51 (m, 8H, Ar-H), 6.97 (m, 3H, Ar-H), 3.76 (s, 3H, OCH_3), 3.69 (s, 3H, OCH_3).

4.4.11. *2-(3,4-Dimethoxyphenyl)-4,5-bis(4-fluorophenyl)-1H-imidazole (**4k**, $C_{23}H_{18}F_2N_2O_2$)*

Cream powder; R_f (in petroleum ether:ethylacetate; 7:3(v/v)): 0.24; U.V ($CHCl_3$) λ_{max}(nm): 340; IR (KBr) $\bar{\nu}$ (cm^{-1}): 3440 (N-H), 1604(C=C), 1504 (C=N), 1228(C-O); ^{1}H NMR (DMSO-d_6, 400 MHz) δ (ppm): 12.9 (s, 1H, N-H), 8.19 (d, 2H, ^3J=8 Hz, Ar-H); 8.05 (m, 4H, Ar-H), 7.78 (t, 2H, ^3J=8 Hz, Ar-H), 7.58 (m, 3H, Ar-H), 4.34 (s, 3H, OCH_3), 4.30 (s, 3H, OCH_3).

4.4.12. *2-(2-naphthyl)-4,5-bis(4-fluorophenyl)-1Himidazole (**4l**, $C_{25}H_{16}N_2F_2$)*

White powder; R_f (in petroleum ether:ethylacetate; 7:3(v/v)): 0.73; U.V ($CHCl_3$) λ_{max}(nm): 352, IR (KBr) $\bar{\nu}$ (cm^{-1}): 3433 (N-H), 1669 (C=C), 1559 (C=N), 1247(C-O); ^{1}H NMR (DMSO-d_6, 400 MHz) δ (ppm): 12.9 (s, 1H, N-H), 8.58 (s, 1H, Ar-H), 8.23 (d, 1H, ^3J=7.2 Hz, Ar-H), 7.94-8.21 (m, 4H, Ar-H)),7.47-7.56 (m, 5H, Ar-H), 7.33 (t, 2H, ^3J=8.4 Hz, Ar-H), 7.16 (t, 2H, ^3J=8.4 Hz, Ar-H).

Acknowledgments

We gratefully acknowledge the financial support from the Research Council of the University of Kashan for supporting this work by Grant (No. 256722/29).

References

1. S. Samai, G.C. Nandi, P. Singh, M.S. Singh, *Tetrahedron*., 2009, **65**, 10155–10161.
2. A. Teimouri, A. Najafi Chermahini, *J Mol. Catal. A: Chem*., 2011, **34**, 639– 45.
3. M. Antolini, A. Bozzoli, C. Ghiron, G. Kennedy, T. Rossi, A. Ursini, *Bioorg. Med. Chem. Lett*., 1999, **9**, 1023-1028.
4. K. Sivakumar, A. Kathirvel, A. Lalitha, *Tetrahedron Lett*., 2010, **51**, 3018–3021.
5. J.C. Lee, J.T. Laydon, P. C. McDonnell, T.F. Gallagher, S. Kumar, D. Green, D. McNulty, M.J. Blumenthal, J.R. Keys, S.W.L. Vatter, J.E. Strickler, M.M. McLaughlin, I.R. Siemens, S.M. Fisher, G.P. Livi, J.R. White, J.L. Adams, P.R. Young, *Nature*., 1994, **372**, 739-746.
6. A.K. Takle, M.J.B. Brown, S. Davies, D.K. Dean, G. Francis, A. Gaiba, A.W. Hird, F.D. King, P.J. Lovell, A. Naylor, A.D. Reith, J.G. Steadman, D.M. Wilson, *Bioorg. Med. Chem. Lett*., 2006, **163**,78-381.
7. R. Schmierer, H. Mildenberger, H. Buerstell, German Patent 361464, 1987; Chem. Abstr. 1988, **108**, 37838.
8. S.E. de Laszlo, C. Hacker, B. Li, D. Kim, M. MacCoss, N. Mantalo, J.V. Pivnichny, L. Colwell, G.E. Koch, M.A. Cascieri, W.K. Hagmenn, *Bioorg. Med. Chem. Lett*., 1999, **96**, 41-646.
9. T. Maier, R. Schmierer, K. Bauer, H. Bieringer, H. Buerstell, B. Sachse, U.S. Patent 4820335, 1989; Chem. Abstr. 1989, **111**, 19494w.
10. J. Heeres, L.J.J. Backx, J.H. Mostmans, J. Van Custem, *J. Med. Chem*., 1979, **22**, 1003-1005.
11. A. Shaabani, A. Rahmati, *J Mol Catal A Chem*., 2006, **249**, 246-248.
12. K. Sivakumar, A. Kathirvel, A. Lalitha, *Tetrahedron Lett*., 2010, **51**, 3018–3021.
13. K.F. Shelke, S.B. Sapkal, S.S. Sonar, B.R. Madje, B.B. Shingate, M.S. Shingare, *Bull Korean Chem Soc*., 2009, **30**, 1057-1060.
14. S.D. Jadhave, N.D. Kokare, S.D. Jadhave, *J Heterocycl Chem.*, 2009, **45**, 1461-1464.
15. H. Weinmann, M. Harre, K. Koeing, E. Merten, U. Tilestam, *Tetrahedron Lett*., 2002, **43**, 593-595.
16. J. Liu, J. Chen, J. Zhao, Y. Zhao, L. Li, H. Zhang, *Synthesis*., 2003, 2661-2666.
17. N.D. Kokare, J.N. Sangshetti, D.B. Shinde, *Synthesis*., 2007, 2829-2834.
18. M.M. Khodaei, K. Bahrami, I. Kavianinia, *J. Chin. Chem. Soc*., 2007, **54**, 829-833.
19. X. Zheng, S. Luo, L. Zhang, J.P. Cheng, *Green Chem*., 2009, **11**, 455–458.
20. A. Maleki, N. Ghamari, M. Kamalzare, *RSC Adv*., 2014, **49**, 416–9423.
21. J. Safari, S.H. Banitaba, S.D. Khalili, *J Mol. Catal. A: Chem*., 2011, **335**, 46-50.
22. G. Chen, B. Fang, *Bioresour. Technol*., 2011, **102**, 2635-2640.
23. (a) M.G. Dekamin, M. Azimoshan, L. Ramezani, Green *Chem*., 2013, **158**, 811–820; (b) J. Zhu, P.C. Wang, M, Lu, *New J. Chem*., 2012, **36**, 2587–2592.
24. S. Wu, H. Ma, X. Jia, Y. Zhong and Z. Lei, *Tetrahedron*., 2011, **67**, 250–256.
25. (a) G.A. Dee, O. Rhode, R. Wachter, *Cosmet. Toiletories*., 2001, **116**, 39–44; (b) K.R. Reddy, K. Rajgopal, C.U. Maheswari, M.L. Kantam, *New J. Chem*., 2006, **30**,1549–1552.
26. R. Mohammadi, M. Zaman Kassaee, *J Mol. Catal. A: Chem*., 2013, **380**, 152– 158
27. A. Zhu, L. Yuan, T. Liao, Int. *J. Pharm*., 2008, **350**, 361–368)
28. Z. Liu, H. Bai, D.D. Sun, *New J. Chem*., 2011, **35**, 137–140.
29. J. Safari, S.D. Khalili, S.H. Banitab, H. Dehghani, *Bull. Korean Chem. Soc*., 2011, **55**, 1-7.
30. J. Safari, S.D. Khalili, M. Rezaei, S.H. Banitab, F. Meshkani, *Monatsh Chem*., 2010, **141**, 1339-1345.
31. S.D. Khalili, Safari, J*PhD Thesis*, Kashan University, kashan, Iran, **2011**.

Figure captions

Table 1: Effect of the amount of Fe_3O_4@chitosan nanoparticles and solvents on the synthesis of compound **4a** under reflux condition.

Table 2: One-pot synthesis of 2,4,5-trisubstituted imidazoles catalyzed by Fe_3O_4@chitosan nanoparticles under reflux condition.

Scheme 1. One-pot synthesis of 2,4,5-trisubstituted imidazoles catalyzed by Fe_3O_4@CS.

Scheme 2. Preparation steps for fabricating heterogeneous Fe_3O_4@CS nanoparticles.

Scheme 3. Plausible mechanism of the reaction.

Fig. 1. IR spectra of (a) chitosan, (b) Fe_3O_4, (c) Fe_3O_4@CS and (d) recovered Fe_3O_4@chitosan.

Fig. 2. XRD patterns of the (a) Fe_3O_4 MNPs, (b) Fe_3O_4@CS nanocomposite and (c) chitosan.

Fig. 3. TGA curves for (a) uncoated MNPs and (b) Fe_3O_4@chitosan nanocomposite.

Fig. 4. SEM morphology of (a) unmodified Fe_3O_4 magnetic nanoparticles, (b) Fe_3O_4@chitosan nanocomposite and (c) Fe_3O_4@chitosan after being used 6 times.

Fig. 5. Magnetization curves for the Fe_3O_4 MNPs and Fe_3O_4@chitosan nanocomposite at room temperature.

Fig. 6. ^{1}H NMR spectra of 2-(4-methoxyphenyl)-4,5-diphenyl-1H-imidazole **(4b)** in (a) Acetone+DMSO-d_6 and (b) Acetone+D_2O.

Fig. 7. Separation of the nanocatalyst from the reaction mixture by an external magnet.

Fig. 8. Fig. 8. Reusability of Fe_3O_4@chitosan for the synthesis of **4a** and **4b.**

Table 1
Effect of the amount of Fe_3O_4@chitosan nanoparticles and solvents on the synthesis of compound **4a** under reflux condition.

Entry	Catalyst (g)	Solvent	Time (h)	Yield (%)
1	-	EtOH	5	15
2	Fe_3O_4@chitosan (0.03)	EtOH	3	60
3	Fe_3O_4@chitosan (0.04)	EtOH	2	72
4	**Fe_3O_4@chitosan (0.05)**	**EtOH**	**2**	**95**
5	Fe_3O_4@chitosan (0.06)	EtOH	2	94
6	Fe_3O_4 (0.05)	EtOH	2	70
7	chitosan (0.05)	EtOH	2	80
8	Fe_3O_4@chitosan (0.05)	MeOH	3	90
9	Fe_3O_4@chitosan (0.05)	Acetonitrile	3	70
10	Fe_3O_4@chitosan (0.05)	Chloroform	5	55
11	Fe_3O_4@chitosan (0.05)	Dichloromethane	5	40

Table 2

One-pot synthesis of 2,4,5-trisubstituted imidazoles catalyzed by Fe_3O_4@chitosan under reflux condition.

Entry	R_1,R_2	R_3	Product	Time (h)	Yield (%)	$mp_{rep}/mp_{lit.}$ (°C)
1	H	H	**4a**	2	95	(271-273) / (270-272) [29]
2	H	p-OMe	**4b**	3	90	(230-231) / (228-231) [29]
3	H	m-OMe, p-OMe	**4c**	2	92	(214-216) / 213-216 [30]
4	H	p-Cl	**4d**	2.5	96	(260-262) / (260-261) [30]
5	H	m-OMe	**4e**	2.5	98	(258-260) / (259-262) [29]
6	H	2-Naphthyl	**4f**	2.5	98	(274-275) / (273-276) [30]
7	H	m-OMe, m-OMe	**4g**	3.5	98	(255-257) / (254-256) [30]
8	OMe	H	**4h**	3	95	(202-204) / (201-203) [29]
9	OMe	p-OMe	**4i**	3.5	90	(184-186) / (183-185) [29]
10	OMe	2-Naphthyl	**4j**	3	95	228-230 / 228-230 [31]
11	F	m-OMe, p-OMe	**4k**	1	98	(206-208) / (207-208) [30]
12	F	2-Naphthyl	**4l**	1	98	273-275 / 273-275 [31]

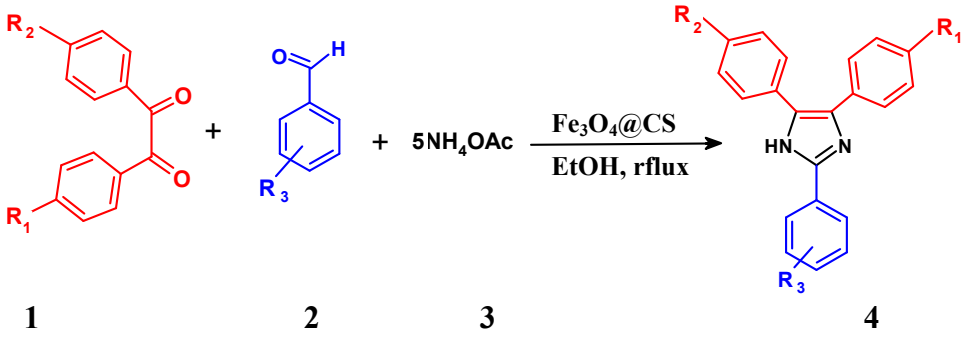

Scheme 2. One-pot synthesis of 2,4,5-trisubstituted imidazoles catalyzed by Fe_3O_4@CS.

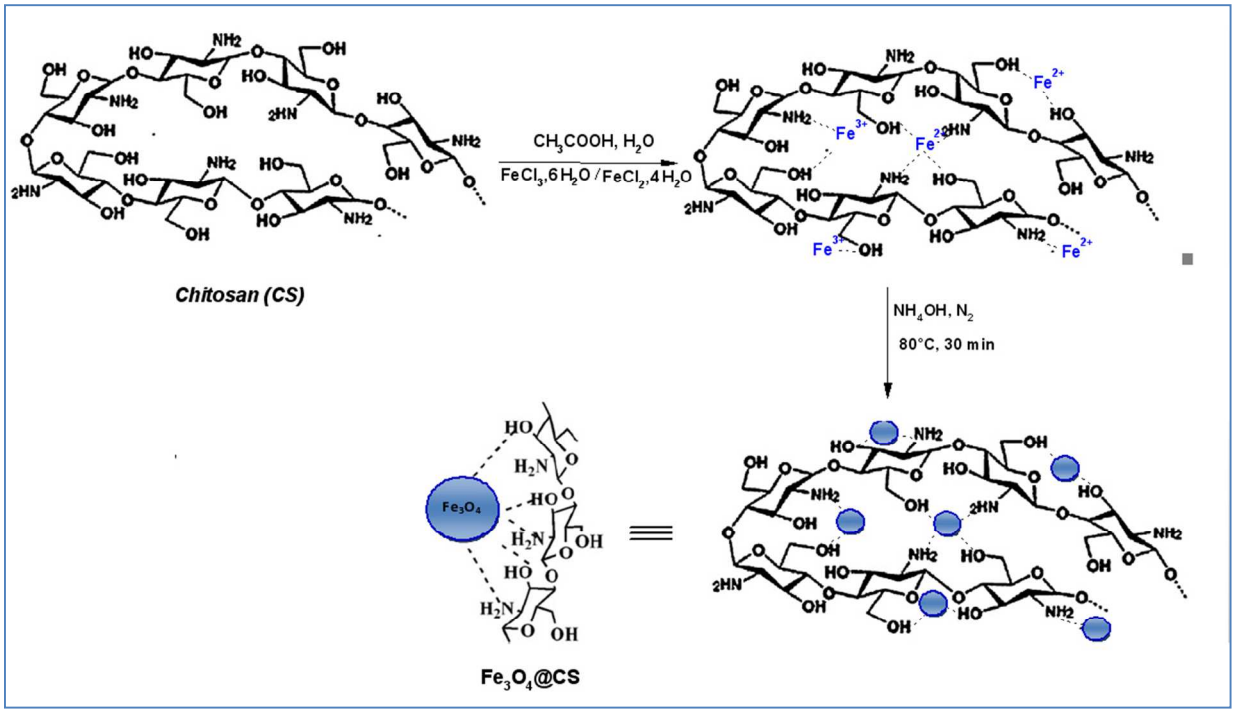

Scheme 3. Preparation steps for fabricating heterogeneous Fe_3O_4@CS nanoparticles.

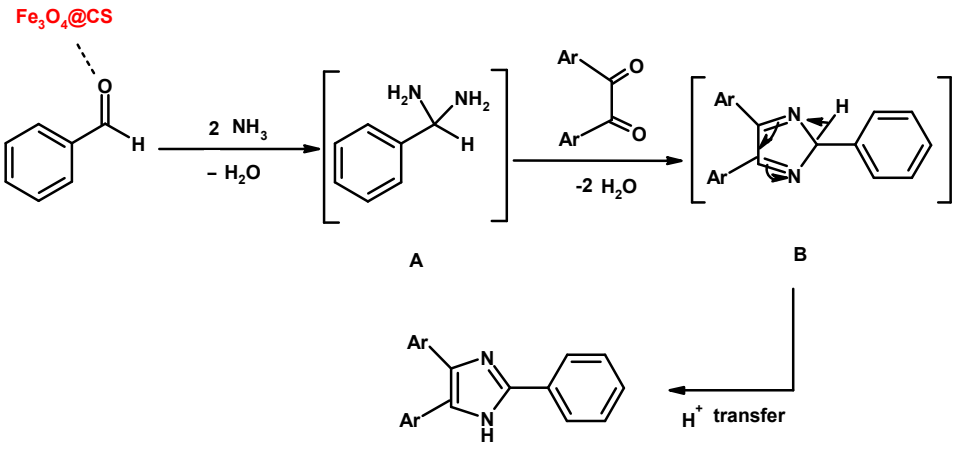

Scheme 4. Plausible mechanism of the reaction.

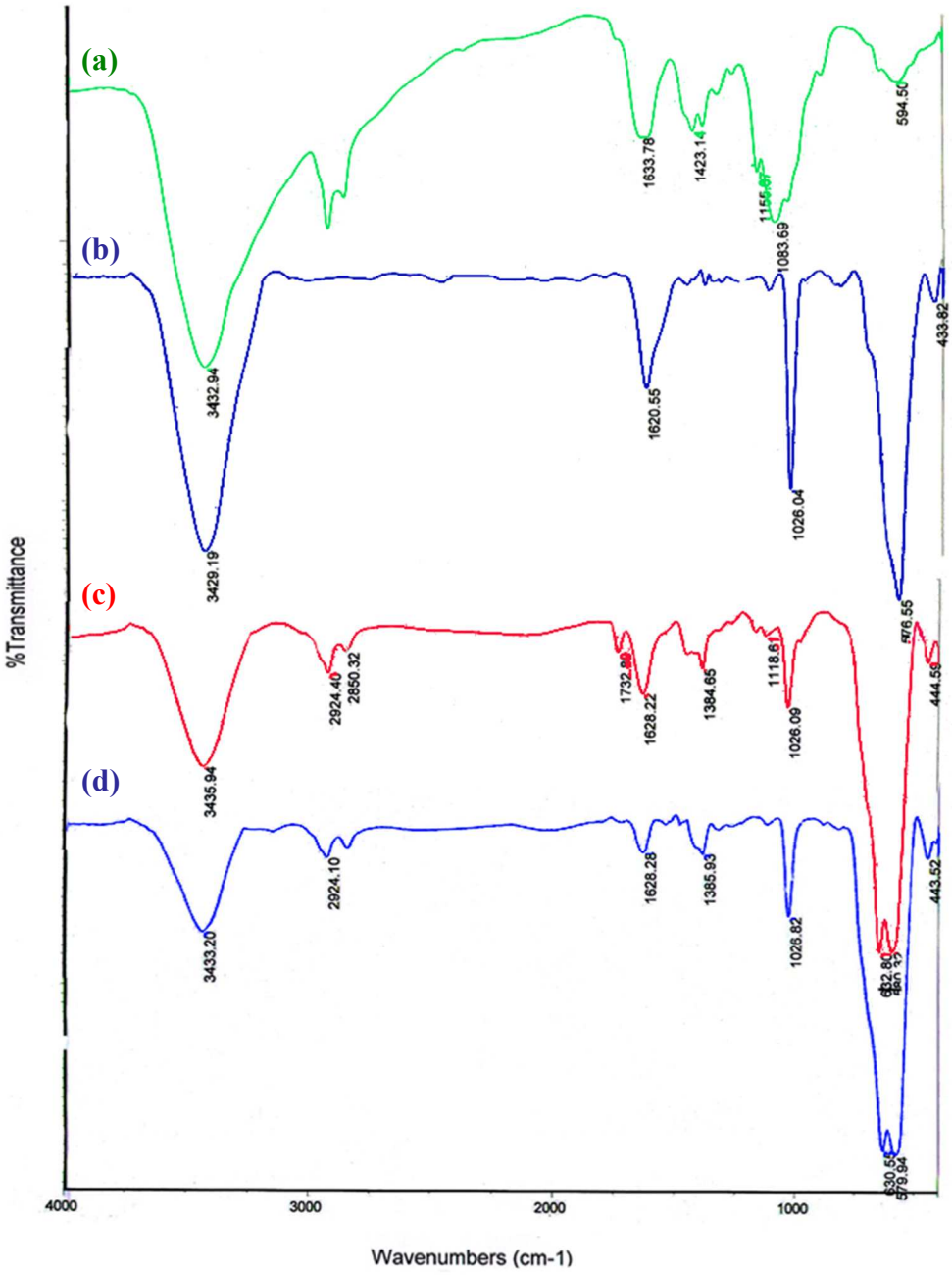

Fig. 1. IR spectra of (a) chitosan, (b) Fe_3O_4, (c) Fe_3O_4@CS and (d) recovered Fe_3O_4@chitosan.

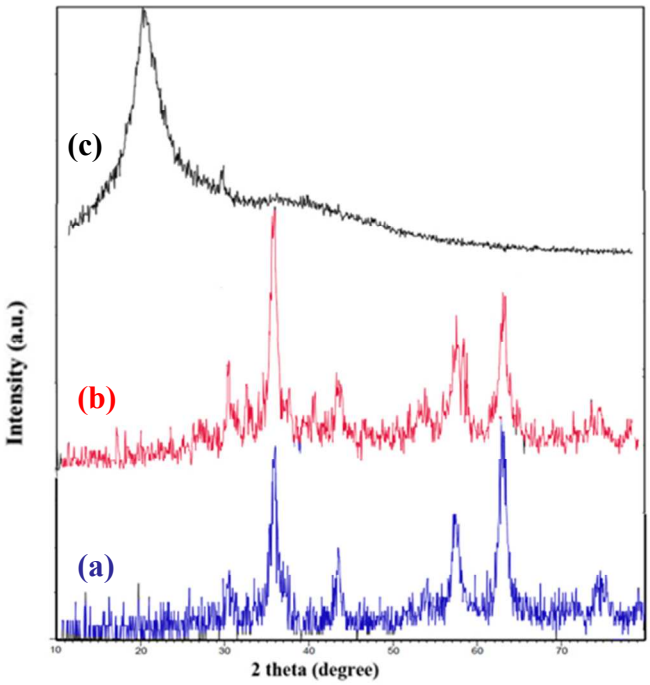

Fig. 2. XRD patterns of the (a) Fe_3O_4 MNPs, (b) Fe_3O_4@CS nanocomposite and (c) chitosan.

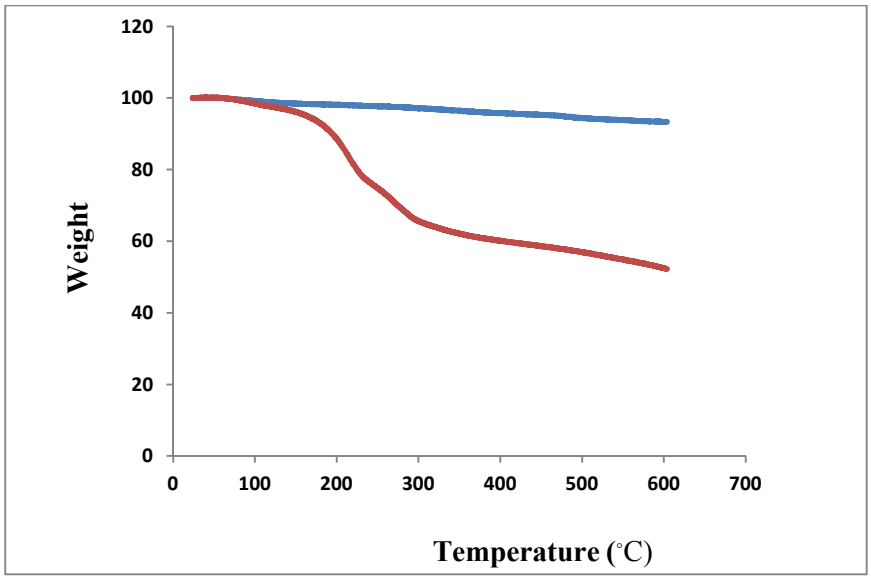

Fig. 3. TGA curves for (a) uncoated MNPs and (b) Fe_3O_4@chitosan nanocomposite.

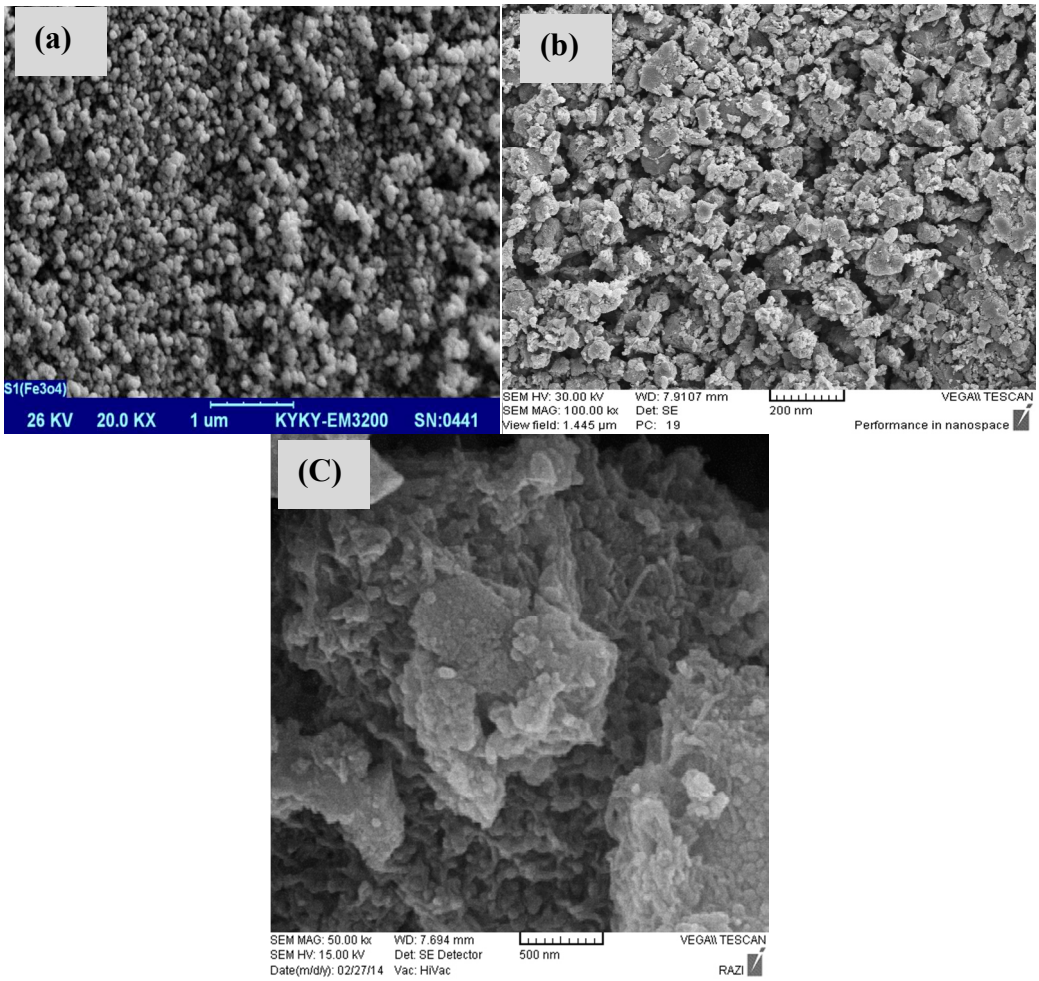

Fig. 4. SEM morphology of (a) unmodified Fe_3O_4 magnetic nanoparticles, (b) Fe_3O_4@chitosan nanocomposite and (c) Fe_3O_4@chitosan after being used 6 times.

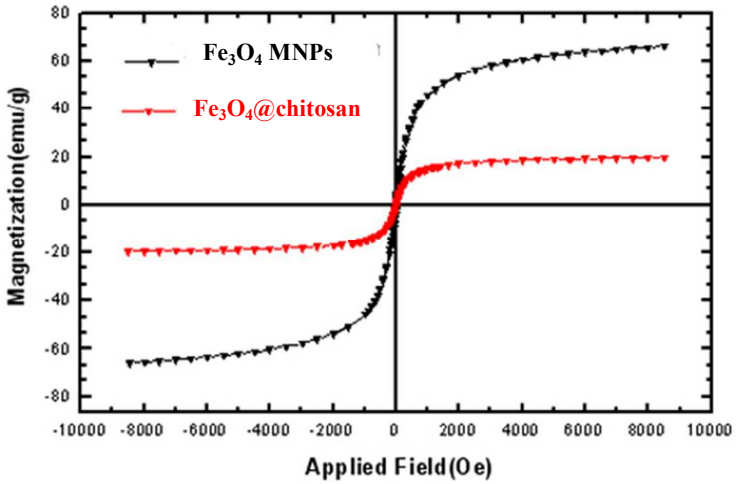

Fig. 5. Magnetization curves for the Fe_3O_4 MNPs and Fe_3O_4@chitosan nanocomposite at room temperature.

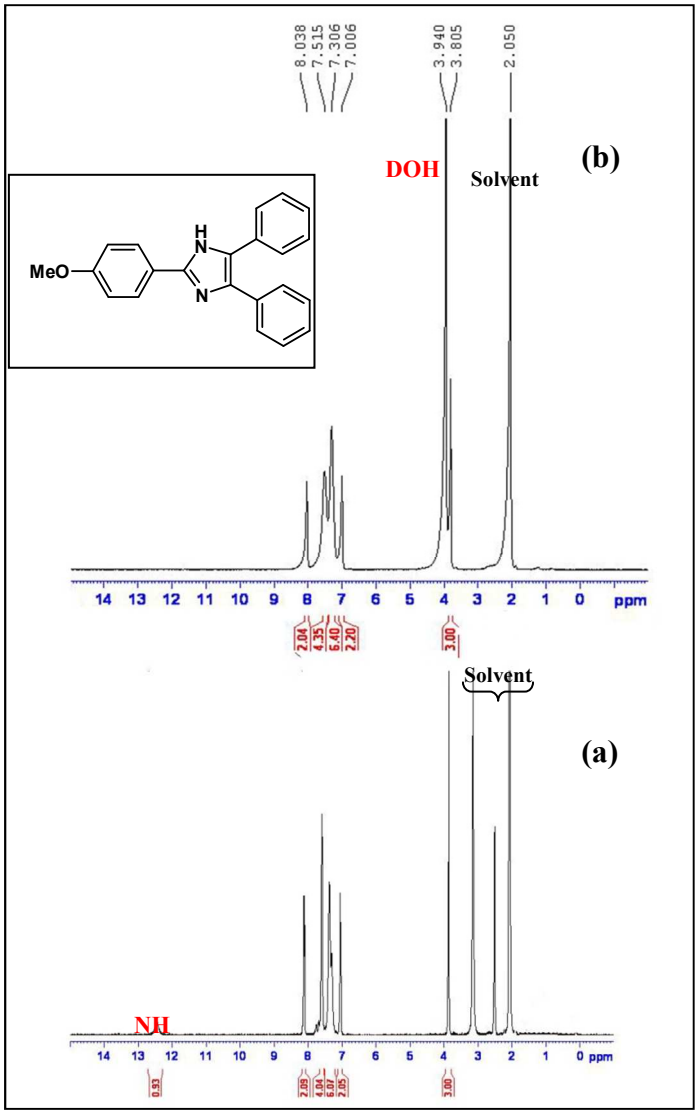

Fig. 6. ^{1}H NMR spectra of 2-(4-methoxyphenyl)-4,5-diphenyl-1H-imidazole **(4b)** in (a) Acetone+DMSO-d_6 and (b) Acetone+D_2O.

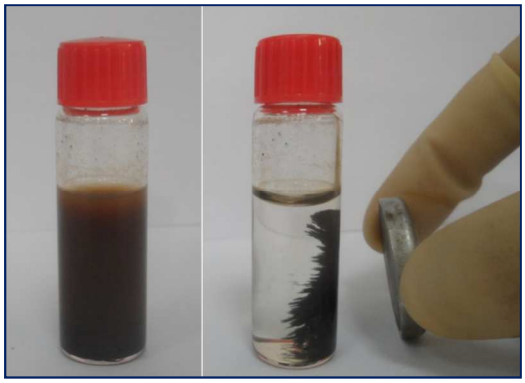

Fig. 7. Separation of the nanocatalyst from the reaction mixture by an external magnet.

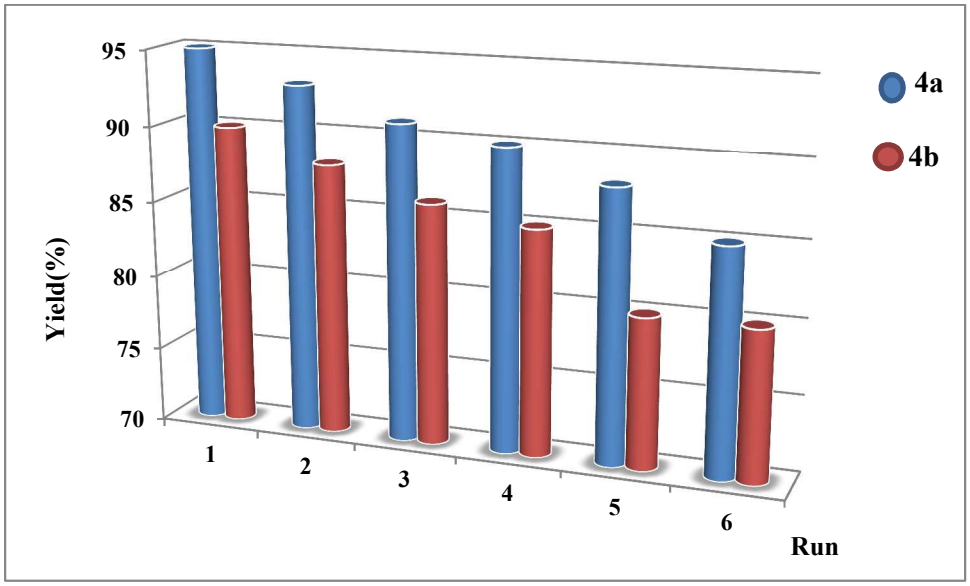

Fig. 8. Reusability of Fe_3O_4@chitosan for the synthesis of **4a** and **4b.**

Graphical Abstract

Fe_3O_4@chitosan nanoparticles: a valuable heterogeneous nanocatalyst for the synthesis of 2,4,5-trisubstituted imidazoles

Zohre Zarnegar, Javad Safari*